IVYSPRING INTERNATIONAL PUBLISHER

International Journal of Biological Sciences

2023; 19(7): 2150-2166. doi: 10.7150/ijbs.80441

Research Paper

Olfactomedin-4 deletion exacerbates DSS-induced colitis through a matrix metalloproteinase-9-dependent mechanism

Xinyu Wang*, Shenghui Chen*, Jinghua Wang, Yishu Chen, Yanjun Guo, Qinqiu Wang, Zhening Liu, Hang Zeng, Chengfu Xu✉

Department of Gastroenterology, the First Affiliated Hospital, Zhejiang University School of Medicine, Hangzhou 310003, China

* Contributed equally

✉ Corresponding author: Chengfu Xu, MD, Department of Gastroenterology, the First Affiliated Hospital, Zhejiang University School of Medicine, 79 Qingchun Road, Hangzhou 310003, China. Telephone: +86-571-87236863; Email: xiaofu@zju.edu.cn. ORCID: 0000-0002-6172-1253

Received: 2022.11.02; Accepted: 2023.03.30; Published: 2023.04.09

Abstract

Background and Aims: Olfactomedin-4 is a glycoprotein that is upregulated in inflamed gastrointestinal tissues. This study aimed to investigate the role and underlying mechanisms of olfactomedin-4 in ulcerative colitis.

Methods: C57BL/6 mice and olfactomedin-4 knockout mice were fed dextran sulfate sodium in drinking water to establish a colitis model. An *in vitro* inflammation model was constructed in HCT116 and NCM460 cells stimulated with lipopolysaccharide. The expression of olfactomedin-4 was detected by Western blotting, immunohistochemistry staining, and qRT–PCR. The differences in the severity of colitis between olfactomedin-4 knockout mice and wild-type mice were compared, and the underlying mechanisms were explored.

Results: Olfactomedin-4 expression was significantly upregulated in colonic tissues of active ulcerative colitis patients and in cellular and mouse models of colitis. Compared with wild-type littermates, olfactomedin-4 knockout mice were more susceptible to dextran sulfate sodium-induced colitis and produced higher levels of proinflammatory cytokines and chemokines. In addition, olfactomedin-4 deficiency significantly promoted intestinal epithelial cell apoptosis and increased intestinal permeability, which was mediated by the p53 pathway. Moreover, olfactomedin-4 directly interacted with and negatively regulated matrix metalloproteinase-9. Inhibiting matrix metalloproteinase-9 significantly decreased colonic p53 expression and ameliorated experimental colitis in olfactomedin-4 knockout mice, while overexpression of matrix metalloproteinase-9 aggravated colitis. Further experiments showed that matrix metalloproteinase-9 regulated p53 through the Notch1 signaling pathway to promote ulcerative colitis progression.

Conclusions: Olfactomedin-4 is significantly upregulated in ulcerative colitis and may protect against colitis by directly inhibiting matrix metalloproteinase-9 and further decreasing p53-mediated apoptosis *via* Notch1 signaling.

Keywords: Ulcerative colitis; olfactomedin-4; matrix metalloproteinase-9; apoptosis

Introduction

Ulcerative colitis (UC) is one of the two major types of inflammatory bowel disease (IBD), which is a chronic intestinal inflammatory disorder characterized by diarrhea, abdominal pain, and rectal bleeding [1]. Accumulating evidence suggests that UC results from multiple causes, including genetics, the environment, microbes, and inappropriate inflammatory responses [1-3]. Dysregulation of immune responses is considered to play a major role in UC development [4, 5]. Various proinflammatory cytokines and

chemokines play a central role in abnormal immune responses [5, 6]. Moreover, intestinal epithelial cells (IECs) provide the first-line defense formed by a physical and biochemical barrier [7]. Excessive apoptosis of IECs [8, 9], breakage of tight junction complexes [10], defects in the mucus layer [11], and any other behaviors leading to a compromised barrier with bacterial invasion may create a vicious cycle exacerbating UC [11-13]. However, the exact pathogenesis of UC is still under investigation.

Olfactomedin-4 (OLFM4, also called GW112 or hGC-1), a 72 kDa glycoprotein belonging to the olfactomedin family, is highly expressed in the small intestine and colon [14, 15]. OLFM4 is widely distributed in cells, including the membrane, cytoplasm, nucleus, and mitochondria [16, 17]. OLFM4 interacts with several other proteins to perform a variety of biological functions, including proliferation, differentiation, apoptosis, and cell adhesion [17, 18]. This molecule also plays an important role in innate immune regulation [19]. In addition, OLFM4 can be secreted into the extracellular space for biological purposes [20]. The expression of OLFM4 is upregulated in the intestinal epithelium of IBD patients, including those with UC and Crohn's disease (CD), but is more significantly upregulated in active UC patients [21]. Previous studies have shown that the OLFM4 protein marks intestinal stem cells [22] and is aberrantly expressed in the inflamed colonic mucosa in UC patients [21, 23]. However, the specific functions of OLFM4 in the colon are still unclear.

Matrix metalloproteinase-9 (MMP9, gelatinases B) is a multidomain enzyme belonging to the MMP family [24]. In addition to the conserved catalytic domain of MMPs, MMP9 contains a unique O-glycosylated domain that can facilitate enzyme flexibility [25]. Strong evidence indicates that MMP9 induces chronic inflammation, aberrant tissue remodeling, and degradation of extracellular matrix (ECM) components [26, 27], which are hallmarks of IBD. The expression of MMP9 was found in the mucosal tissue of IBD patients, most prominently in actively inflamed areas [28, 29]. The serum neutrophil gelatinase B-associated lipocalin and MMP9 (Ngal-MMP9) complex is suggested as a surrogate marker to assess mucosal healing in UC and Crohn's disease patients [30, 31]. However, the upstream and downstream molecules involved in the mechanisms of MMP9 in UC remain unclear.

The multifunctional gene p53 acts as a tumor suppressor to determine cell fate and prevent the expansion of damaged cells [32]. Increased expression of p53 has been detected in UC patients and animal colitis models [33, 34]. Studies have shown that p53 is required for IEC apoptosis [35], which requires the expression of p53 and p53 upregulated modulator of apoptosis (PUMA) [8, 36]. Several groups have revealed that p53 deficiency could protect against acute intestinal inflammation [33, 36]. The regulatory effect of MMP9 on p53 has been reported and involves Notch signaling [37, 38]. However, the involvement of MMP9- and p53-mediated apoptosis in ulcerative colitis has not been fully explored.

In this study, we aimed to explore the role and underlying regulatory mechanism of OLFM4 in ulcerative colitis.

Materials and methods

Human tissue

Human colonic mucosa specimens from 17 active UC patients and 8 healthy controls were obtained during endoscopic examinations at the Department of Gastroenterology, the First Affiliated Hospital, Zhejiang University School of Medicine. The diagnosis of UC was based on accepted clinical criteria, including typical symptoms, as well as endoscopic, histologic, and radiographic diagnoses [39]. This study was approved by the Clinical Research Ethics Committee of the First Affiliated Hospital, Zhejiang University School of Medicine (approval no. 2022354).

Animal treatment

OLFM4 knockout mice (*Olfm4*-/-) on a C57BL/6 background were generated through CRISPR technology by Beijing ViewSolid Biotechnology (Beijing, China). Wild-type littermate male C57BL/6 mice were purchased from Zhejiang Experimental Animal Centre (Hangzhou, China). Mice were acclimated for 7 days in an animal room with air-conditioned specific pathogen-free (SPF) conditions at 23± 2 °C with a 12 h light/dark cycle before experimentation. The protocol to develop chemically induced acute colitis in C57BL/6 mice or *Olfm4*-/- mice was described previously [40]. The male mice (8 weeks old) received 35 g/L dextran sulfate sodium (DSS, 36–50 kDa, MP Biomedicals, Santa Ana, CA) in their drinking water for 6 days, while control mice received autoclaved water. The body weight, the presence of occult or gross blood per rectum, and stool consistency were assessed daily for the calculation of the disease activity index score, as previously described [41]. Entire colons were collected from the experimental mice and fixed flat in 40 g/L formaldehyde for 48 h. Colon sections (5 mm thick) were embedded in paraffin and stained with hematoxylin and eosin. The inflammation scores were determined as previously described [41, 42]. All animal studies were approved by the Animal Care and Use Committee of the First Affiliated Hospital,

Zhejiang University School of Medicine (approval No. 20191097).

Adeno-associated virus (AAV) administration

Recombinant AAV serotype 9 was selected, according to the literature, to mediate relatively high efficiency gene delivery to intestinal epithelial cells [43, 44]. AAV carrying shMMP9 (AAV-shMMP9) or control vector (AAV-shNC) was generated and purified as described previously 45. Then, male 8-week-old wild-type (WT) and *Olfm4*-/- mice (n = 7–10/group) received a single intravenous dose of 2 × 1011 AAV-shMMP9 or AAV-shNC in a volume of 150 µl through tail vein injection according to previous studies [43, 46]. All mice were housed under a standard 12-hour light/dark cycle and fed a standard rodent chow diet and autoclaved tap water ad libitum. After 1 week, colitis was induced by DSS in drinking water for 6 days.

Inhibition of Notch signaling

Difluorophenacetyl-L-alanyl-S-phenylglycine t-butyl ester (DAPT, Sigma–Aldrich) was used to inhibit the Notch signaling pathway 47. HCT116 cells were treated with 1 µmol/ml DAPT. Age- and sex-matched C57B6 WT and *Olfm4*-/- mice (n=10/group) were obtained by intraperitoneal injection of DAPT five consecutive times during DSS drinking to inhibit Notch signaling. The *in vivo* effects of Notch inhibitors in various mouse disease models have been well studied [38, 48, 49]. We chose 10 µmol/kg DAPT as described in previous studies, while the controls received vehicle alone [38]. DAPT was solubilized in DMSO and diluted in phosphate-buffered saline (PBS) containing 0.01% (v/v) Tween 80 and 0.5% (w/v) hypromellose (GlpBio, Montclair, CA) [38].

Cell culture and *in vitro* model

The human colorectal adenocarcinoma cell line HCT116, human embryonic kidney 293T cells, and normal colonic epithelial cell line NCM460 (Institute of Biochemistry and Cell Biology, China Academy of Sciences, Shanghai, China) were used for experiments. HCT116 and 293T cells were cultivated in Dulbecco's modified Eagle's medium (DMEM, Gibco Life Technologies, Eggenstein, Germany), and NCM460 cells were cultured in Roswell Park Memorial Institute (RPMI)-1640 medium. The cells were cultured in medium with 100 ml/L fetal bovine serum (FBS, Invitrogen, Carlsbad, CA) and 10 ml/L penicillin–streptomycin (Sigma–Aldrich, St. Louis, MO) in a humidified atmosphere at 37 °C and 50 mL/L CO2. Cells were exposed to lipopolysaccharide (LPS, 1 µg/ml) (Sigma–Aldrich, St. Louis, MO) to establish the *in vitro* inflammation model [50, 51].

Gene expression measurements

mRNA was isolated from cells or tissues using RNAiso Plus (TaKaRa, Otsu, Japan). Prime Script RT Master Mix (TaKaRa) was used to generate cDNA from mRNA. Quantitative real-time PCR was performed using TB Green Premix Ex Taq II (TaKaRa) on a 7500 Fast Real-Time PCR system (Applied Biosystems, Foster City, CA). For the specific primer sequences, see Supplementary Table S1.

Cell transfection

The siRNA oligonucleotides and overexpression plasmids of OLFM4 were purchased from RiboBio (Guangzhou, China). The siRNA, plasmids and corresponding negative controls (at a final concentration of 5 nM) were transfected into cells using Lipofectamine 3000 (Invitrogen) according to the manufacturer's protocol [52]. Cells were transfected with siRNAs for 24 h or plasmid DNA for 6 h and then exposed to LPS for another 24 h.

Western blot assays

Protein was isolated from cells and mouse distal colon tissue by RIPA lysis buffer (Applygen Technologies, Beijing, China) containing protease and phosphatase inhibitors (Pierce Biotechnology, Rockford, IL). Western blotting was carried out as previously described. The protein (20 µg/sample) was separated on an 80 g/L-100 g/L SDS–PAGE gel and transferred to a polyvinylidene difluoride membrane (0.2 mm pore; Millipore, Darmstadt, Germany). Membranes were preincubated with 50 g/L nonfat powdered milk in TBST for 1.5 h, followed by incubation with specific primary antibodies at 4 °C overnight. The primary antibodies are listed in Supplementary Table S2. Signals were detected by HRP-conjugated secondary antibodies (Santa Cruz, CA), and densitometric analysis was performed using ImageJ software (Version 1.51).

Enzyme-linked immunosorbent assay (ELISA)

The protein levels of cytokines and chemokines were tested by ELISAs as previously described [53]. Serum IL-1β, IL-6, MCP1, and ICAM1 levels were measured using commercially available ELISA kits (Mouse IL1β ELISA Kit, KE10003, Proteintech; Mouse IL6 ELISA kit, KE10007, Proteintech; Mouse MCP1 ELISA Kit, KE10006, Proteintech; Mouse ICAM1 ELISA Kit, KE10063 Proteintech) following the manufacturer's instructions.

Immunohistochemistry (IHC)

For IHC, after blocking with 100 g/L normal goat serum (ZSGB-BIO, Beijing, China) in PBS (pH

7.5), tissue sections were incubated with primary antibodies against OLFM4 (dilution: 1:200, Cell Signaling Technology, Danvers, MA) overnight at 4 °C. Tissue sections were stained with secondary antibodies (dilution: 1:1000, ZSGB-BIO, Beijing, China) for 1 h in an incubator maintained at 37 °C. Immunoreactivity was detected by using a DAB kit (ZSGB-BIO).

Terminal deoxynucleotidyl transferase-mediated deoxyuridine triphosphate nick-end labeling (TUNEL) staining

For detection of apoptosis, sections of tissue were stained by TUNEL with a cell death detection kit (Roche, Indianapolis, IN) as described previously [54]. Sections were counterstained with DAPI. Fluorescence images were captured by confocal microscopy (Olympus Corporation, Japan). The number of TUNEL-positive epithelial cells was quantified, and the percentage of apoptotic cells was calculated from eight enlarged photomicrographs of the colon as previously reported [33, 36].

Fluorescein isothiocyanate (FITC)-dextran permeability assay

Intestinal permeability was assessed by oral administration of FITC-labeled dextran (MW 4,000; Sigma–Aldrich) as previously described [55]. After the withdrawal of food overnight, all mice were gavaged with FITC-dextran (60 mg/100 g of body weight) 4 h before sacrifice. The serum was then collected, and the FITC-dextran level in the serum was measured with a fluorescence spectrophotometer with emission and excitation wavelengths of 488 nm and 520 nm, respectively.

RNA sequencing

Total RNA was extracted using TRIzol (TaKaRa) according to the manufacturer's protocol. Preparation of the library and transcriptomic sequencing were carried out using the Illumina HiSeq ×Ten (Novogene Bioinformatics Technology). Mapping of 100-bp paired-end reads to genes was performed using HTSeq software (version 0.6.0), and fragments per kilobase of transcript per million fragments mapped (FPKM) were also analyzed.

Statistical analysis

Statistical analyses were performed, and all graphs were generated with GraphPad Prism software version 8.2.0 using one-way analysis of variance (ANOVA). All data are expressed as the mean ± standard deviation (SD) from at least three independent experiments. P values less than 0.05 were considered statistically significant.

Ethics Approval

This study was approved by the Clinical Research Ethics Committee of the First Affiliated Hospital, Zhejiang University School of Medicine. The experimental procedures were performed in accordance with the approved guidelines of the Ethics Committee. All animal studies were approved by the Animal Care and Use Committee of the First Affiliated Hospital, Zhejiang University School of Medicine and were administered in accordance with the Chinese guidelines for the care and use of laboratory animals.

Results

OLFM4 is highly expressed in inflamed but not normal colon tissue and cells

To investigate the potential association of OLFM4 with UC, we analyzed OLFM4 protein expression in colon tissues from active UC patients. Compared with the healthy controls, the UC patients showed significantly higher colonic expression of OLFM4, as indicated by immunohistochemistry staining (Figure 1A). We also found that OLFM4 expression was significantly increased at both the mRNA and protein levels in LPS-stimulated HCT116 and NCM460 cells (Figure 1B and 1C; Figure S1A and S1B). Moreover, we established a DSS-induced mouse model of acute colitis (Figure 1D; Figure S1C and S1D) and found that OLFM4 levels were significantly increased in the inflammatory area of the colon (Figure 1D). qRT–PCR and Western blotting further confirmed that OLFM4 was highly expressed in the distal colon of the DSS-treated mice but barely expressed under normal conditions (Figure 1E and 1F). These findings suggested a potential association of OLFM4 with UC.

Olfm4 deficiency exacerbates inflammation both *in vitro* and *in vivo*

To explore the function of OLFM4 in colitis, we assessed the effects of OLFM4 knockdown or overexpression on LPS-stimulated inflammation in HCT116 cells. As determined by qRT–PCR, *Olfm4* expression in HCT116 and NCM460 cells was successfully inhibited by *Olfm4* siRNA and significantly increased by the overexpression plasmids (Figure S2A-S2D). Inhibition of *Olfm4* accelerated LPS-stimulated inflammation, while overexpression of *Olfm4* decreased the production of LPS-stimulated inflammatory cytokines and chemokines, including interleukin-6 (Il6), Il1β, monocyte chemoattractant protein-1 (Mcp1), and intercellular adhesion molecule-1 (Icam1) (Figure 2A and 2B; Figure S2E). Icam1 is a downstream factor of the nuclear factor

(NF)-κB pathway [56], which plays an important role in colitis [57]. We found that knocking down *Olfm4* significantly increased the phosphorylation of the NF-κB subunit p65 and the IκB kinase (IKK) complex in LPS-stimulated cells (Figure 2C; Figure S2F). In contrast, *Olfm4* overexpression significantly decreased LPS-induced NF-κB pathway activation (Figure 2D).

To further explore the *in vivo* function of *Olfm4* in colitis, we generated *Olfm4*-/- mice and established a mouse model of acute colitis by adding 35 g/L DSS to the drinking water (Figure 2E; Figure S3A). We found that body weight (Figure S3B), colon length (Figure S3C), and H&E staining (Figure 2F) all indicated more severe and extensive colitis in the *Olfm4*-/- mice than in the WT littermates. The phosphorylated levels of p65, nuclear transport of p65, and the IKK complex were also markedly increased in the colons of the DSS-treated *Olfm4*-/- mice compared with those in the WT controls (Figure 2G). The *Olfm4*-/- mice also had significantly higher colonic mRNA expression and serum levels of proinflammatory cytokines and chemokines, including IL-1β, IL-6, MCP1, and ICAM1, than the WT mice after 6 days of DSS challenge (Figure 2H and 2I). These results suggest that *Olfm4* deficiency exacerbates colitis both *in vitro* and *in vivo*.

Olfm4 deficiency promotes IEC apoptosis and increases intestinal permeability

We performed next-generation RNA sequencing to explore the regulatory mechanisms of OLFM4 in colitis. As expected, numerous differentially expressed transcripts were observed in the colon of the DSS-treated *Olfm4*-/- mice compared with the DSS-treated WT mice. Gene set enrichment analysis (GSEA) identified a specific role of *Olfm4* in the apoptosis pathway (Figure 3A). Because excessive IEC apoptosis is closely associated with increased intestinal barrier permeability and deteriorated UC symptoms [8, 9], we assessed whether *Olfm4* affects IEC apoptosis and regulates intestinal barrier integrity. We found that the *Olfm4*-/- mice showed more TUNEL-positive apoptotic cells in the colon than the WT mice upon DSS challenge (Figure 3B). We also observed a threefold increase in the serum FITC–dextran levels of the *Olfm4*-/- mice after 6 days of DSS challenge compared with the DSS-treated WT mice (Figure 3C). Moreover, the levels of cleaved caspase 3 and caspase 7, two activated forms of the most important downstream caspases in the apoptosis pathway, were significantly higher in the *Olfm4*-/- mice than in the WT mice after DSS challenge (Figure 3D). Other apoptosis-related factors, including cleaved poly (ADP-ribose) polymerase (PARP) and

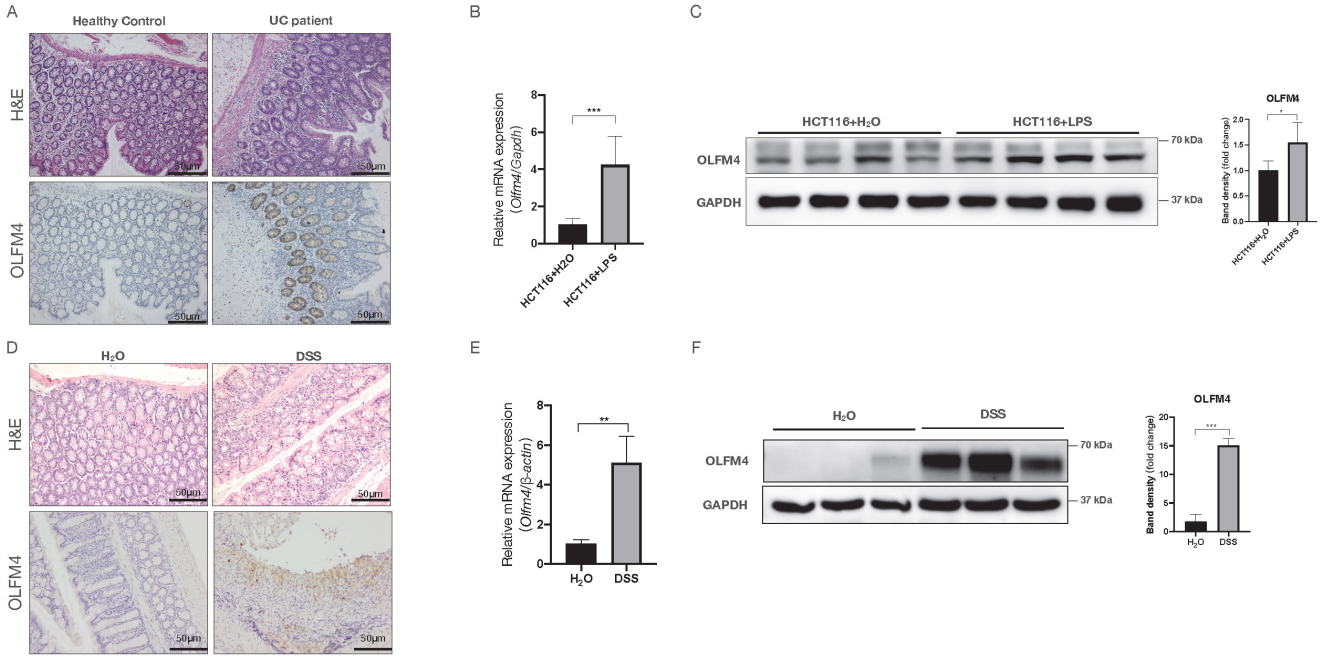

Figure 1. OLFM4 expression is upregulated in colitis both *in vivo* and *in vitro*. (A) H&E-stained images of colon tissues from UC patients and healthy controls (above). Immunohistochemistry of OLFM4 is described in the figure below (scale bar: 50 μm). **(B)** qRT–PCR analysis of *Olfm4* mRNA levels in LPS-stimulated HCT116 cells. Data are the means ± SDs. $n = 6$. ***$P<0.001$. **(C)** Western blotting analysis of OLFM4 protein levels in LPS-stimulated HCT116 cells. The OLFM4 protein level was quantified using ImageJ software analysis. *$P<0.05$. **(D)** H&E-stained images of colon sections from WT mice (above). Immunohistochemistry of OLFM4 is described in the figure below (scale bar: 50 μm). **(E)** *Olfm4* mRNA levels were measured in distal colons by qRT–PCR. Data are the means ± SDs. $n = 5$-8. **$P<0.01$. **(F)** The protein level of OLFM4 was measured in distal colons by Western blots and quantified by ImageJ software. ***$P<0.001$.

B-cell lymphoma 2 (BCL2)-associated X protein (BAX), were also increased, while the antiapoptotic factor BCL2 was significantly decreased in the DSS-treated *Olfm4*-/- mice compared with the WT controls (Figure 3D and 3E). Additionally, we examined other cell death mechanisms, including necroptosis and ferroptosis. *Olfm4* deficiency did not affect these processes (Figure S4A and S4B). These findings suggested that *Olfm4* deficiency promotes IEC apoptosis and increases intestinal permeability in the mice with DSS-induced colitis.

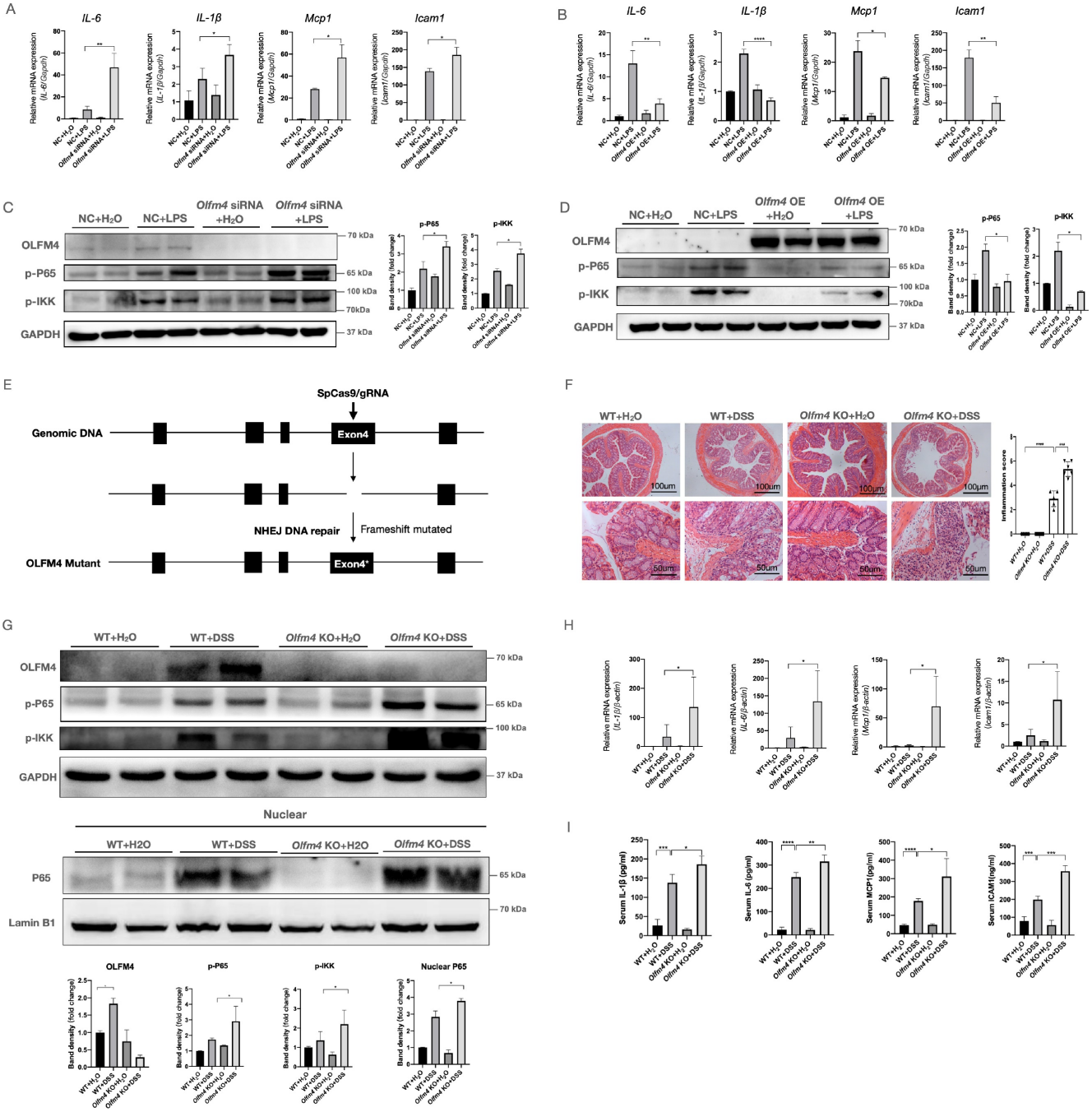

Figure 2. Deletion of *Olfm4* exacerbates colitis. (A) The mRNA levels of *Il6*, *Il1β*, *Mcp1*, and *Icam1* were measured in HCT116 cells by qRT–PCR. Data are the means ± SDs. $n = 6$. **P*<0.05, ***P*<0.01. **(B)** The mRNA levels of *Il6*, *Il1β*, *Mcp1*, and *Icam1* were measured in HCT116 cells by qRT–PCR. Data are the means ± SDs. $n = 6$. **P*<0.05, ***P*<0.01, ****P*<0.001. **(C)** The protein levels of OLFM4, p-P65, and p-IKK were measured in HCT116 cells by Western blotting and quantified by ImageJ software. **P*<0.05. **(D)** The protein levels of OLFM4, p-P65, and p-IKK were measured in HCT116 cells by Western blot and quantified by ImageJ software. **P*<0.05. **(E)** *Olfm4*$^{-/-}$ mice were generated through CRISPR technology. **(F)** Colon sections from WT mice and *Olfm4* KO mice were stained with H&E (left), and inflammation scores (right) were determined to assess injury and inflammation. ****P*<0.001, *****P*<0.0001. **(G)** The protein levels of OLFM4, p-P65, and p-IKK and the nuclear level of P65 were measured in the distal colons of WT mice and *Olfm4*$^{-/-}$ mice by Western blotting and quantified by ImageJ software. **P*<0.05. **(H)** The mRNA levels of *Il1β*, *Il6*, *Mcp1*, and *Icam1* were measured in distal colons by qRT–PCR. Data are the means ± SDs. $n = 5$-8. **P*<0.05. **(I)** The protein levels of IL-1β, IL-6, MCP1, and ICAM1 were measured in serum by ELISAs. Data are the means ± SDs. $n = 5$-8. **P*<0.05, ***P*<0.01, ****P*<0.001, *****P*<0.0001.

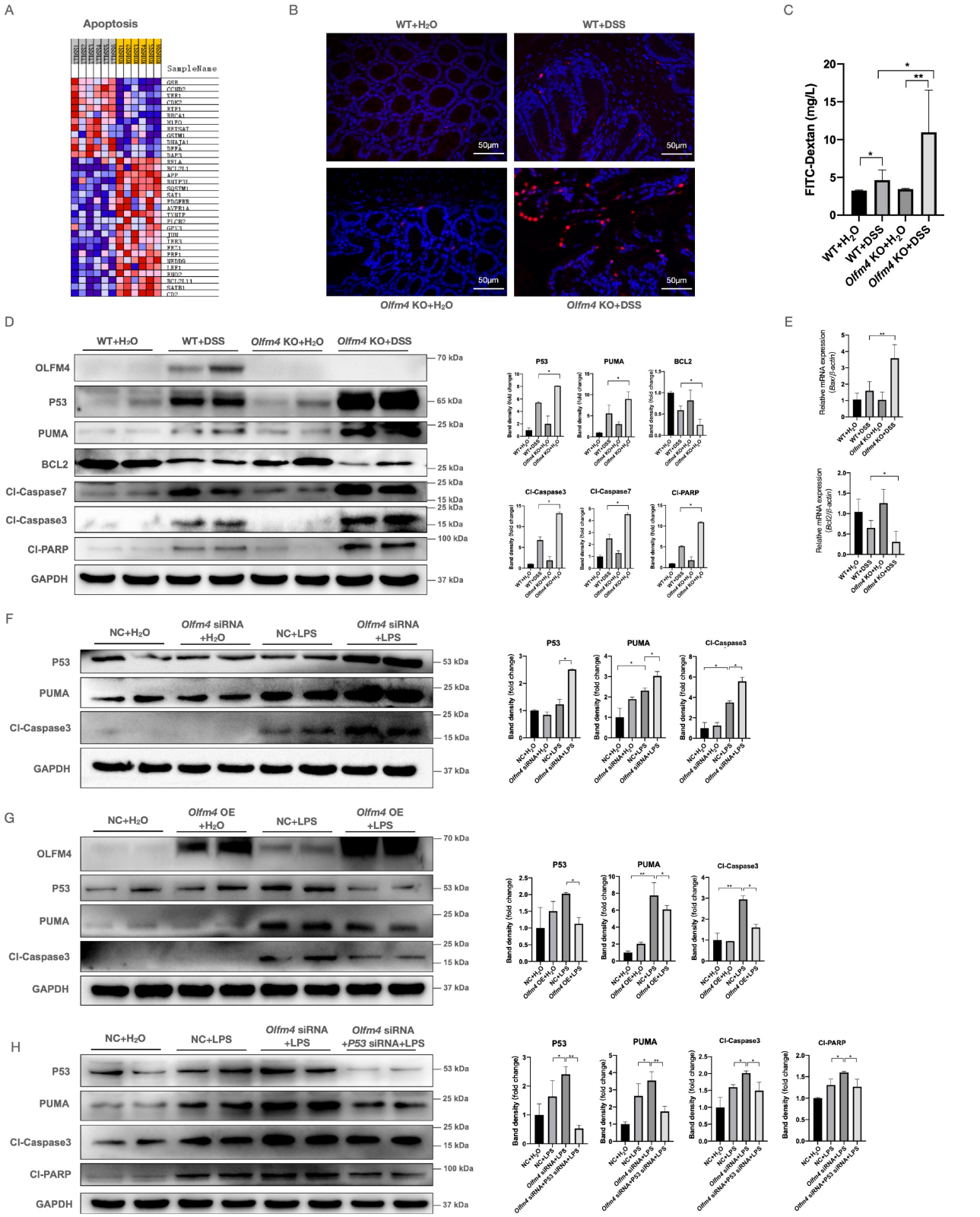

Figure 3. *Olfm4* deficiency promotes p53-mediated IEC apoptosis. (A) RNA sequencing detected differentially expressed mRNAs in DSS-treated WT and *Olfm4*$^{-/-}$ mice. **(B)** TUNEL-positive apoptotic cells in the colons of WT and *Olfm4*$^{-/-}$ mice upon DSS treatment. **(C)** Serum FITC–dextran levels of DSS-treated WT and *Olfm4*$^{-/-}$ mice. n = 5-8. **P*<0.05, ***P*<0.01. **(D)** Representative WB analyses (left) and quantification (right) of the protein levels of genes related to p53-mediated apoptosis in mice. **P*<0.05. **(E)** The mRNA levels of *Bax* and *Bcl2* were measured in distal colons by qRT–PCR. Data are the means ± SDs. n = 5-8. **P*<0.05, ***P*<0.01. **(F)** Representative western blot analyses (left) and quantification (right) of the protein levels of genes related to p53-mediated apoptosis in HCT116 cells. **P*<0.05. **(G)** Representative western blot analyses (left) and quantification (right) of the protein levels of genes related to p53-mediated apoptosis in HCT116 cells. **P*<0.05, ***P*<0.01. **(H)** Representative WB analyses (left) and quantification (right) of the protein levels of genes related to p53-mediated apoptosis in LPS-induced HCT116 cells simultaneously transfected with *Olfm4* siRNA and p53 siRNA. **P*<0.05, ***P*<0.01.

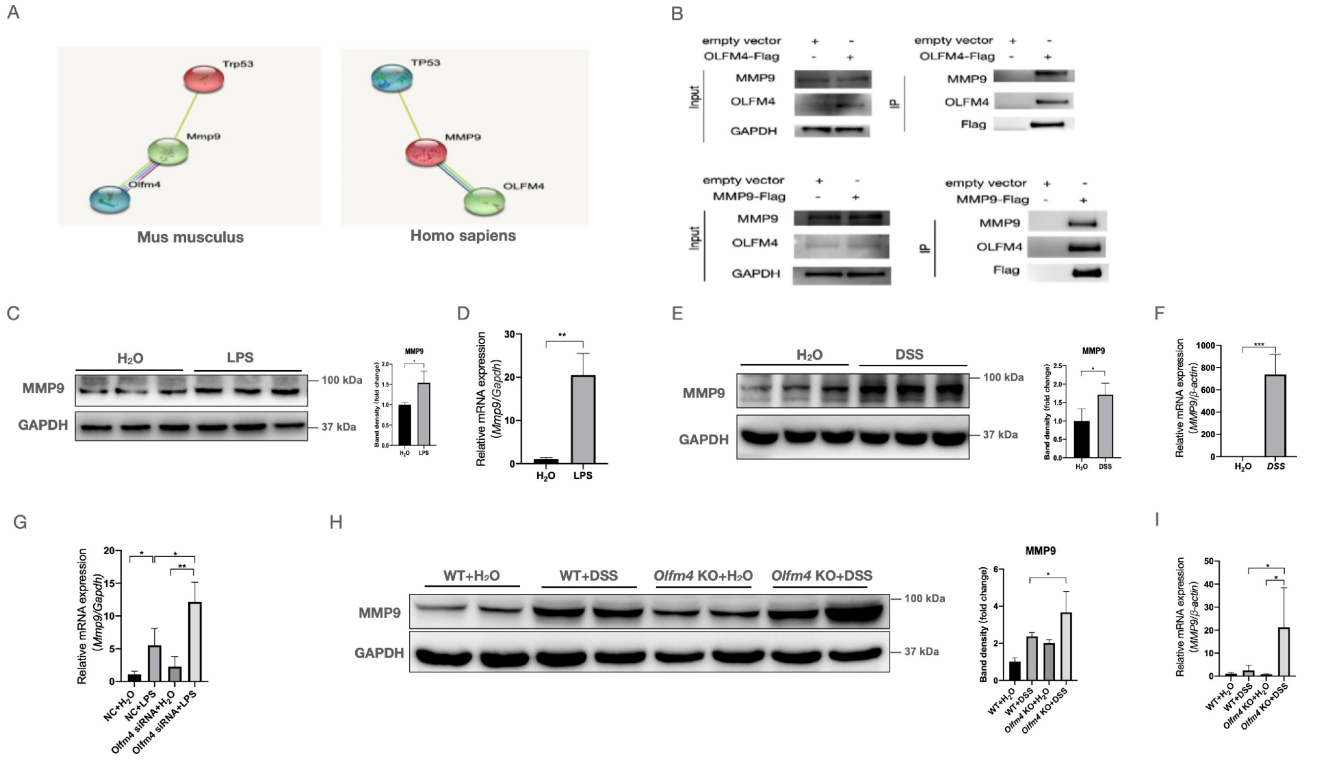

Figure 4. MMP9 mediates the interaction between OLFM4 and p53. (A) The relationship predicted by the STRING database (http://string-db.org/). **(B)** Co-IP analysis confirmed the interaction between OLFM4 and MMP9 in 293T cells. **(C)** The protein levels of MMP9 in HCT116 cells measured by Western blots. **P*<0.05. **(D)** The mRNA expression of MMP9 in HCT116 cells. Data are the means ± SDs. *n* = 6. ***P*<0.01. **(E)** The protein levels of MMP9 in the colons of DSS-treated WT mice compared with control mice. **P*<0.05. **(F)** The mRNA expression of *Mmp9* in mouse colons. Data are the means ± SDs. *n* = 6. ****P*<0.001. **(G)** The mRNA expression of MMP9 was detected in HCT116 cells by qRT–PCR. Data are the means ± SDs. *n* = 6. **P*<0.05, ***P*<0.01. **(H)** The protein levels of MMP9 were detected in the colons of DSS-treated WT or *Olfm4*$^{-/-}$ mice by Western blotting analysis. **P*<0.05. **(I)** The mRNA expression of *Mmp9* was detected in the colons of DSS-treated WT or *Olfm4*$^{-/-}$ mice by qRT–PCR. Data are the means ± SDs. *n* = 6. **P*<0.05.

Olfm4 deficiency promotes IEC apoptosis by enhancing p53 activation

We further investigated the mechanism by which OLFM4 regulates IEC apoptosis. P53 is a key regulator of apoptosis, the cell cycle, and senescence [58], and it is involved in IBD pathogenesis by regulating cell cycle arrest and apoptosis [12, 36, 42]. Here, we found that *Olfm4* deficiency significantly upregulated the colonic protein p53 and its downstream factor, PUMA, in DSS-treated mice (Figure 3D). We also found that knockdown of *Olfm4* significantly increased the expression of p53 and PUMA in LPS-stimulated HCT116 cells (Figure 3F), while overexpression of *Olfm4* inhibited p53 pathway activation (Figure 3G). Moreover, siRNA-mediated knockdown of p53 inhibited the excessive activation of the apoptosis pathway caused by *Olfm4* knockdown in LPS-stimulated HCT116 cells (Figure 3H). These results indicate that *Olfm4* deficiency may promote IEC apoptosis by enhancing p53 activation and may thereby exacerbate colitis.

MMP9 mediates the regulatory effect of OLFM4 on p53 in colitis

To investigate whether OLFM4 regulates p53 directly or indirectly, we searched the STRING database (http://string-db.org/) and predicted MMP9 to mediate the interaction between OLFM4 and p53 (Figure 4A). Our coimmunoprecipitation (co-IP) analysis confirmed the interaction between OLFM4 and MMP9 in 293T cells and HCT116 cells (Figures 4B and S5A). We also observed that the expression of MMP9 was dramatically upregulated at both the mRNA and protein levels in the cellular and mouse models of colitis (Figure 4C-4F), and knockout of *Olfm4* further upregulated the expression of MMP9 in LPS-stimulated cells and in the colon of DSS-treated mice (Figure 4G-4I; Figure S5B).

Moreover, we found that MMP9 is closely associated with apoptosis-related genes (Figure S6). Deficiency of Mmp9 significantly inhibited the inflammatory response and p53-mediated apoptosis pathway in the LPS-stimulated *Olfm4* knockdown HCT116 and NCM460 cells (Figure 5A and 5B; Figure S7A-S7C). In contrast, overexpression of Mmp9 significantly reversed the suppression of the inflammatory response and p53-mediated apoptosis pathway in the LPS-stimulated *Olfm4*-overexpressing HCT116 cells (Figure S7D-S7G).

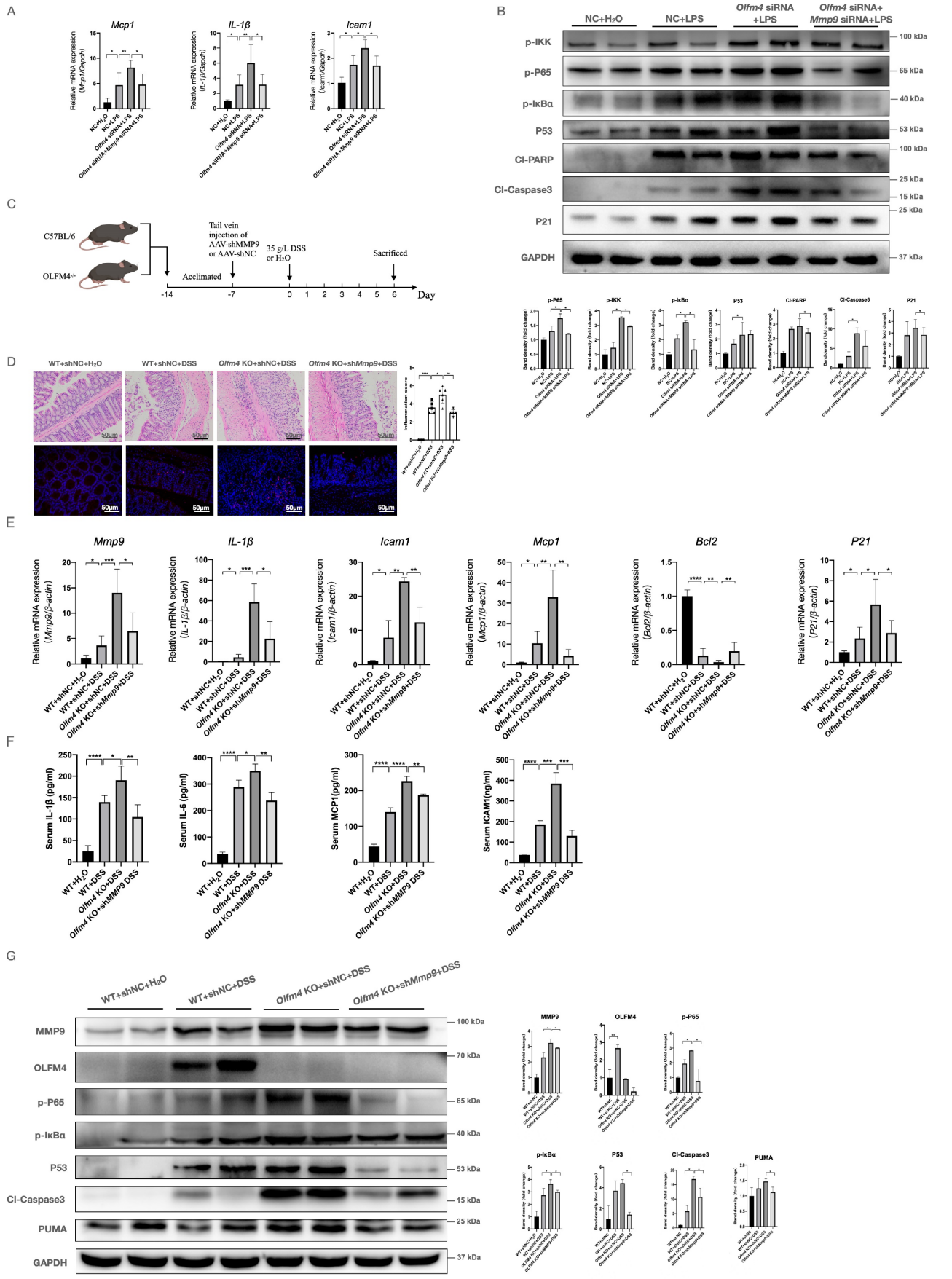

Figure 5. MMP9 mediates the regulatory effect of OLFM4 on p53. (A) The mRNA expression of *Mcp1*, *Il16*, and *Icam1* was detected in HCT116 cells by qRT–PCR. Data are the means ± SDs. $n = 6$. *P<0.05, **P<0.01. **(B)** Representative western blot analyses and quantification of the protein levels of genes related to the inflammatory

response and p53-mediated apoptosis in HCT116 cells. *P<0.05. **(C)** AAV-shMMP9 or AAV-shNC was injected into *Olfm4*$^{-/-}$ mice or WT littermates one week before DSS treatment. **(D)** Colon sections were stained with H&E (left, scale bar: 50 μm), and inflammation scores (right) were calculated to assess injury and inflammation. TUNEL staining showed apoptotic cells in the colons of mice (scale bar: 50 μm). *P<0.05, **P<0.01, ****P<0.0001. **(E)** The mRNA expression of *Mmp9*, *Mcp1*, *Il1β*, *Icam1*, *Bcl2*, and *P21* was measured by qRT–PCR. Data are the means ± SDs. n = 6. *P<0.05, **P<0.01, ***P<0.001, ****P<0.0001. **(F)** The protein levels of IL-1β, IL-6, MCP1, and ICAM1 were measured in serum by ELISAs. Data are the means ± SDs. *n* = 5-8. *P<0.05, **P<0.01, ***P<0.001, ****P<0.0001. **(G)** The protein levels of genes related to the inflammatory response and p53-mediated apoptosis were detected by Western blotting and quantified by ImageJ software. *P<0.05.

To explore whether MMP9 mediated the regulatory effects of OLFM4 on colitis in mice, we transfected *Olfm4*-/- mice and WT littermates with recombinant adeno-associated virus-shMMP9 (AAV-shMMP9) or control vectors (AAV-shNC) through tail vein injection (Figure 5C; Figure S8A-S8D). AAV-mediated inhibition of Mmp9 significantly ameliorated DSS-induced clinical and pathological manifestations of colitis in the *Olfm4*-/- mice (Figure 5D and 5E; Figure S8E and S8F). Inhibition of MMP9 also significantly decreased the inflammatory response, IEC apoptosis, and p53 expression in the DSS-challenged *Olfm4*-/- mice (Figure 5D-5G). These results suggest that MMP9 mediates the regulatory effects of OLFM4 on p53 in colitis.

OLFM4 targets MMP9 and further regulates p53 via Notch1

As a matrix metalloproteinase, MMP9 functions outside the cell 27. The effects of MMP9 on p53 need to be further clarified. Although MMP9 cannot directly interact with p53 (Figure S9A), previous studies have shown that MMP9 can regulate intestinal epithelial homeostasis through Notch signaling [37, 38, 59]. The GSEA scores for Notch signaling positively correlated with MMP9 only in the DSS-treated *Olfm4*-/- mice and not in the WT mice (Figure S9B). Notch signaling could provide support for p53 activation [38, 60]. Notch1, together with p53, drives an antiproliferative process of differentiation, senescence, and apoptosis [60]. The Notch signaling pathway is a critical regulator of mucosal inflammation and intestinal epithelial cell fate determination [59, 61]. Here, we found that knockdown of *Olfm4* significantly increased the mRNA and protein levels of cleaved NOTCH1 and its downstream marker hairy and enhancer of split-1 (HES1) in HCT116 cells (Figure 6A and 6B). Knockdown of Mmp9 significantly suppressed Notch signaling in the *Olfm4* knockdown HCT116 cells regardless of LPS stimulation (Figure 6C-6G). Inhibition of MMP9 also significantly decreased colonic expression of NOTCH1 and HES1 in the DSS-treated *Olfm4*-/- mice (Figure 6H). These findings suggest that OLFM4 targets MMP9 and thereby further regulates the expression of NOTCH1.

To further confirm whether NOTCH1 is essential for OLFM4 to regulate colitis, we inhibited the Notch signaling pathway by DAPT47. *In vitro*, 1 μmol/ml DAPT treatment effectively inhibited the Notch signaling pathway (Figure S10A) but did not affect the expression of OLFM4 or MMP9 (Figure S10A) in HCT116 cells. Inhibiting Notch signaling significantly reversed the deteriorating effects of *Olfm4* knockdown on inflammation and p53-mediated apoptosis in LPS-stimulated HCT116 cells (Figure 7A and 7B). *In vivo*, we injected 10 μmol/kg DAPT into WT and *Olfm4*-/- mice every day during the experimental period to inhibit Notch1 (Figure 7C, Figure S10B). We found that DAPT significantly repressed the activity of the p53-mediated apoptosis pathway (Figure 7D-7F) and alleviated DSS-induced colitis in *Olfm4*-/- mice (Figure 7D-7G; Figure S10C-S10E).

OLFM4 regulates UC in a p53-dependent manner

To verify whether *Olfm4* is directly involved in the regulation of UC in a p53-dependent manner, we re-expressed *Olfm4* or knocked down p53 expression in *Olfm4*-/- mouse colons by trial vein injection of AAV. We found that the re-expression of *Olfm4* significantly relieved weight loss and colon shortening in the DSS-treated *Olfm4*-/- mice (Figure S11A and S11B). Histological analyses confirmed that re-expression of *Olfm4* significantly ameliorated colitis in the DSS-treated *Olfm4*-/- mice (Figure 8A). Re-expression of *Olfm4* also significantly reversed the upregulation of proinflammatory cytokine and chemokine expression in the colon and serum (Figure 8B and 8C) and increased p-P65 and MMP9 protein levels caused by *Olfm4* deficiency (Figure 8D). In addition, apoptosis and intestinal permeability were improved by *Olfm4* re-expression (Figure 8A, 8D, and 8E). These findings demonstrated that re-expression of *Olfm4* ameliorated DSS-induced colonic inflammation and apoptosis in *Olfm4*-/- mice.

Finally, we found that knocking down p53 significantly ameliorated DSS-induced colitis in *Olfm4*-/- mice (Figure 8F-8H; Figure S11C and S11D). Downregulation of p53 significantly decreased the inflammatory response, IEC apoptosis, and intestinal permeability in the DSS-challenged *Olfm4*-/- mice (Figure 8F and 8I). Consistently, p53 deficiency ameliorated LPS-induced inflammation in Oflm4 knockdown cells *in vitro* (Figure 8J). These results suggest that p53 mediates the regulatory effects of OLFM4 in colitis.

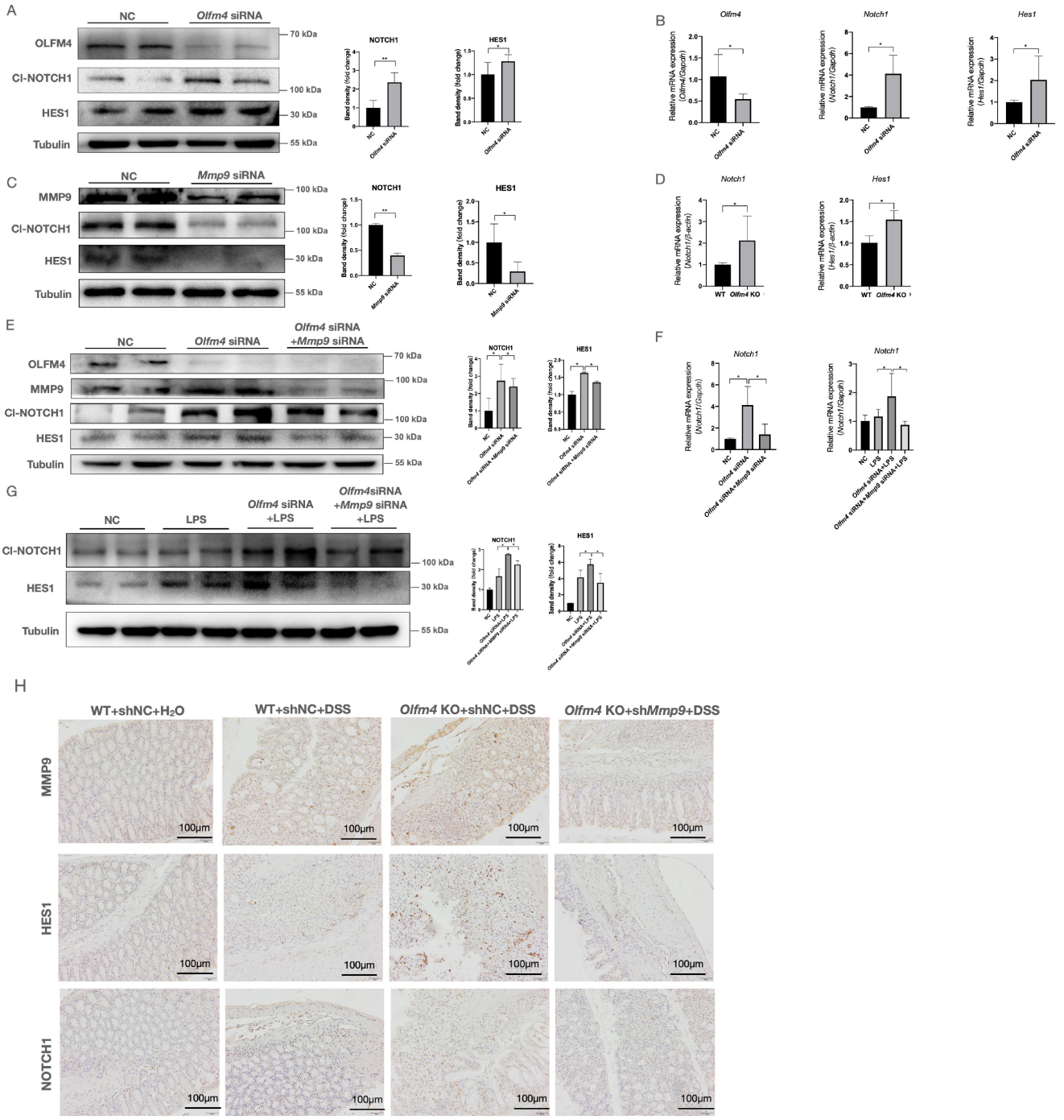

Figure 6. OLFM4 targets MMP9 and further regulates p53 *via* Notch1. (A) The protein levels of Cl-NOTCH1 and HES1 increased in OLFM4 knockdown HCT116 cells. **P*<0.05, ***P*<0.01. **(B)** The mRNA expression of *Olfm4, Notch1*, and *Hes1* was measured by qRT–PCR. Data are the means ± SDs. *n* = 6. **P*<0.05. **(C)** The protein levels of Cl-NOTCH1 and HES1 decreased in MMP9 knockdown HCT116 cells. **P*<0.05, ***P*<0.01. **(D)** The mRNA expression of *Notch1* and *Hes1* was detected in mouse colons. Data are the means ± SDs. *n* = 6. **P*<0.05. **(E)** The protein levels of OLFM4, MMP9, Cl-NOTCH1, and HES1 detected in HCT116 cells by Western blots and quantified by ImageJ software. **P*<0.05. **(F)** The mRNA expression of *Notch1* was measured by qRT–PCR. Data are the means ± SDs. *n* = 6. **P*<0.05. **(G)** The protein levels of Cl-NOTCH1 and HES1 detected in HCT116 cells by Western blots and quantified by ImageJ software. **P*<0.05. **(H)** The protein levels of NOTCH1 and HES1 detected by IHC in mouse colons.

Together, our results suggested that OLFM4 protects against colitis in a p53-dependent manner by targeting MMP9 via Notch1 signaling.

Discussion

This study focused on the role and regulatory mechanisms of OLFM4 in colitis. We observed a significant increase in *Olfm4* expression in active UC patients and in cellular and mouse models of colitis. We also observed that *Olfm4*-/- mice are more vulnerable to DSS-induced colitis, and OLFM4 regulates colitis through p53-mediated IEC apoptosis. Furthermore, we found that Mmp9 is the key factor connecting *Olfm4* and its downstream pathways through the *Olfm4*-Mmp9-Notch1-p53 axis in colitis.

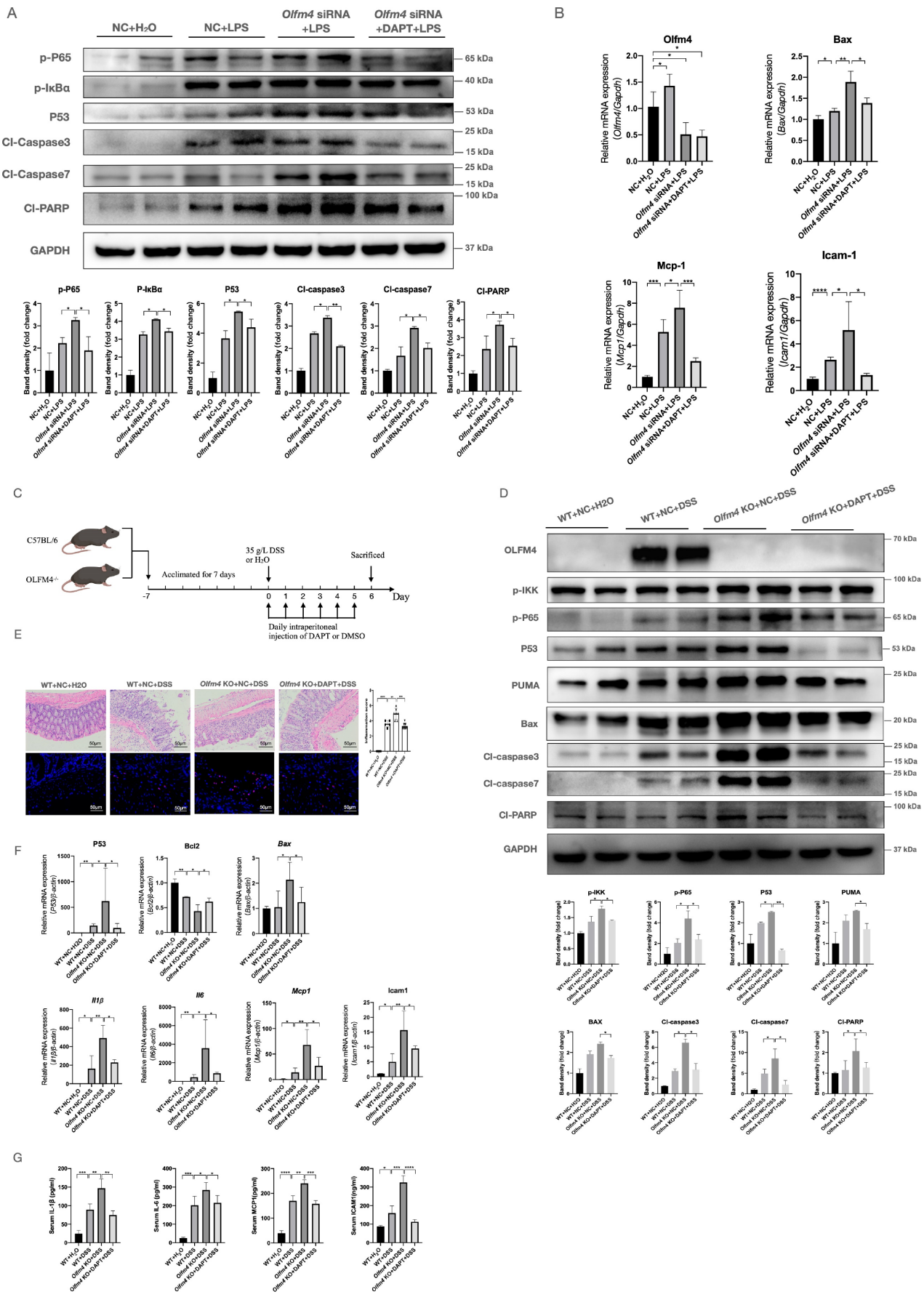

Figure 7. Inhibiting Notch1 could inhibit the regulatory effect of OLFM4 in colitis. (A) The protein levels of genes related to the inflammatory response and p53-mediated apoptosis detected in HCT116 cells. **P*<0.05, ***P*<0.01. **(B)** The mRNA expression of *Olfm4, bax, Mcp1*, and *Icam1* was measured by qRT–PCR. Data are the means

± SDs. n = 6. *P<0.05, **P<0.01, ***P<0.001, ****P<0.0001. **(C)** Mice were injected with DAPT or DMSO every day during the experimental period. **(D)** Representative western blot analyses and quantification of the protein levels of genes related to the inflammatory response and p53-mediated apoptosis detected in distal colons. *P<0.05, **P<0.01. **(E)** Colon sections were stained with H&E (left, scale bar: 50 μm), and inflammation scores (right) were calculated to assess injury and inflammation. TUNEL staining showed apoptotic cells in the mouse colons (scale bar: 50 μm). **P<0.01, ***P<0.001, ****P<0.0001. **(F)** The mRNA expression of *p53, Bcl2, Bax, Il1β, Il6, Mcp1*, and *Icam1* was detected in the distal colons by qRT–PCR. Data are the means ± SDs. n = 6. *P<0.05, **P<0.01. **(G)** The protein levels of IL-1β, IL-6, MCP1, and ICAM1 were measured in serum by ELISAs. Data are the means ± SDs. n = 6. *P<0.05, **P<0.01, ***P<0.001, ****P<0.0001.

Previous studies have reported aberrant expression of *Olfm4* in UC patients [21, 23] but have not determined whether the increase is a cause or a consequence of the disease, nor have they investigated the effects and mechanisms of *Olfm4* in UC. We first used more samples than previous studies and detected OLFM4 levels in different segments to confirm that OLFM4 is upregulated in the colonic mucosa of patients with UC. Then, we constructed animal models and cell models to verify the effects of OLFM4 in UC and conducted more in-depth mechanistic studies. The DSS-induced colitis model exhibits several characteristics of human UC, including diarrhea, severe rectal bleeding, weight loss, and infiltration by granulocytes [62]. This model has been one of the most extensively used models to study the contribution of innate immune mechanisms in colitis [63]. Thus, we chose a DSS-induced acute colitis model to confirm the expression change in *Olfm4*. The expression of OLFM4 was very low in the colon of normal mice, which was consistent with previous studies 11, but it was markedly upregulated in experimental colitis. The induction of *Olfm4* expression coincided with the increased severity of inflammation, as demonstrated by the pathological score evaluated by people who were blinded to the group division. *In vitro*, we observed *Olfm4* upregulation induced by LPS stimulation in the HCT116 cell line, which is commonly used for UC research [42, 64]. These data implicate *Olfm4* in the disease progression of colitis.

To better define the role of endogenous *Olfm4* in the development of UC, we established *Olfm4*-/- mice. Interestingly, compared with their WT littermates, *Olfm4*-/- mice showed increased susceptibility to DSS-induced colitis. These data indicate that *Olfm4* plays an inhibitory role in the development of colitis under certain inflammatory stimuli. We also found that *Olfm4* deletion leads to an enhanced immune response and inflammation in the progression of colitis, characterized by enhanced expression of complement Il-1β, Il-6, and Mcp-1 and activation of the NF-κB pathway. NF-κB is an upstream regulator of Mcp1 [56], Il-1β, Il-6 [65] and C3 [66], which can in turn activate NF-κB. Activation of the NF-kB pathway is strongly induced in inflamed tissue from IBD patients [67]. In addition, we found that *Olfm4* deficiency promotes IEC apoptosis characterized by enhanced expression of cleaved caspase 3 and cleaved caspase 7 and more TUNEL-positive cells. Beyond apoptosis, other cell death mechanisms, including necroptosis and ferroptosis, also play a key role in the pathogenesis of intestinal injury [68]. In contrast to the core apoptotic effectors, the genetic deletion of *Olfm4* did not affect the key necroptotic and ferroptotic machinery, including GPX4, RIPK1, RIPK3 and MLKL [69, 70]. OLFM4 is a robust marker for intestinal stem cells [71]. In addition to its stem cell properties, it has many roles in different diseases, including anti-inflammation, apoptosis, cell adhesion and proliferation [15], which are more relevant to this study. Previous studies have described the proinflammatory effect of OLFM4 in colon adenocarcinoma, but this study focused on the occurrence of adenocarcinoma, which is very different from ulcerative inflammation [72]. In our study, we believe that *Olfm4* is upregulated in the inflammatory state to protect against the development of colitis. We not only confirmed the anti-inflammatory and antiapoptotic roles of OLFM4 in UC but also elucidated its downstream mechanism.

Previous studies have revealed the effect of p53 on epithelial cell apoptosis [33, 36], which was significantly activated in *Olfm4*-/- mice after DSS treatment. The results inspired us to determine whether *Olfm4* can act as an upstream molecule of p53 as an apoptosis regulator in UC. In this study, we found that the p53 protein level was increased in the *Olfm4*-deficient mice and regulated by *Olfm4 in vitro*. We discovered that p53 inhibition could rescue the effect caused by *Olfm4* deficiency. However, there is no direct connection between p53 and *Olfm4*. After searching for potential *Olfm4*-interacting proteins and p53-interacting proteins in the STRING database, we found that Mmp9, an ECM enzyme known to be associated with IBD [27, 28], might be a key factor linking *Olfm4* with p53. Mmp9 is elevated in the intestinal tissue of patients with IBD, and previous studies have reported the role of Mmp9 in the intestinal barrier [73]. However, its specific mechanism and its relationship with *Olfm4* have not been studied. Further experiments confirmed our hypothesis that *Olfm4* regulates p53-mediated apoptosis through Mmp9. We first validated the interaction between *Olfm4* and Mmp9. Then, we verified that the interaction between them was required for the function of OLFM4 in IBD.

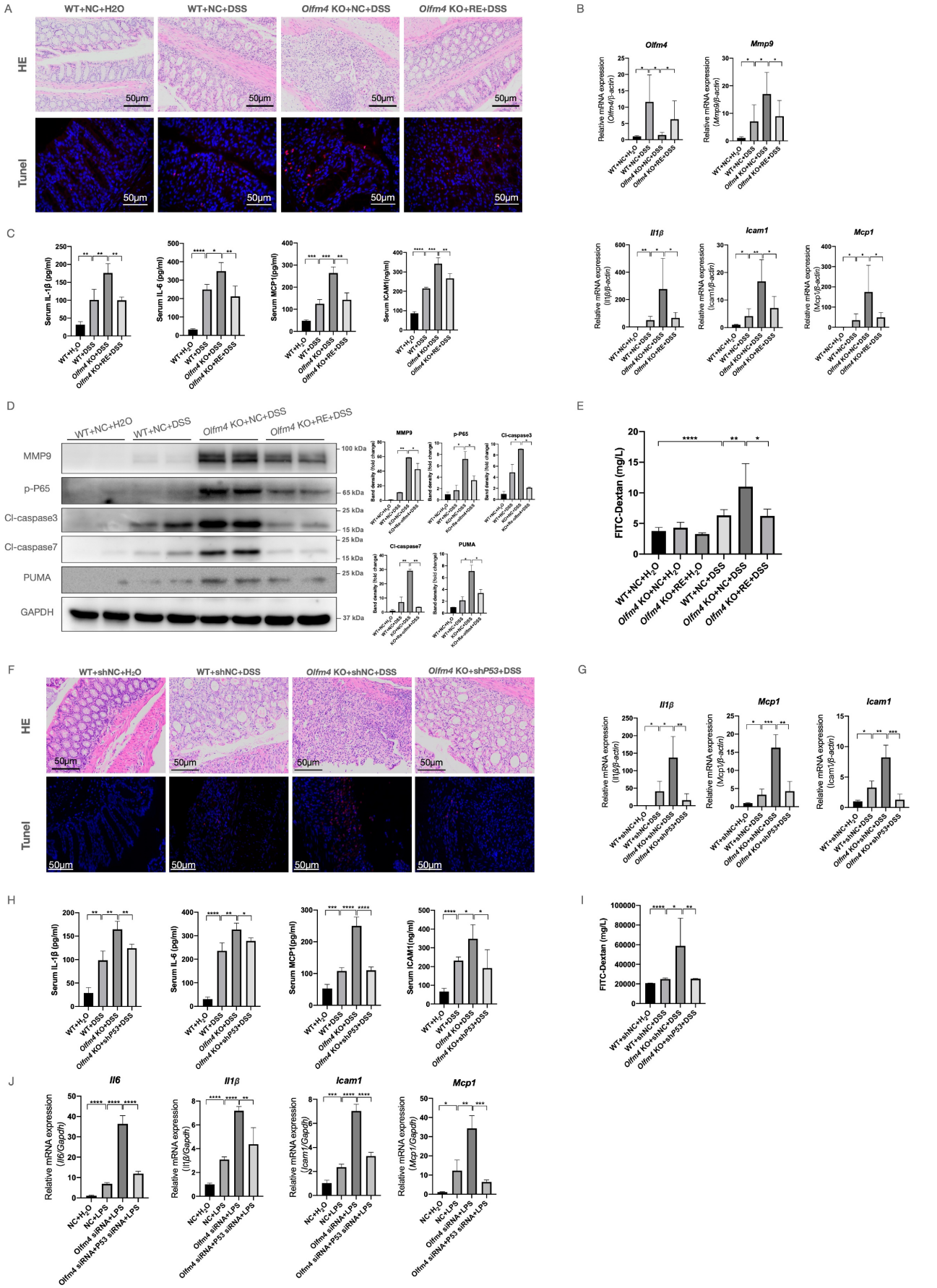

Figure 8. OLFM4 regulates UC in a p53-dependent manner. (A) Colon sections were stained with H&E (scale bar: 50 μm) to assess injury and inflammation. TUNEL staining showed apoptotic cells in the mouse colons (scale bar: 50 μm). **(B)** The mRNA expression of *Olfm4*, *Mmp9*, *Il16*, *Icam1*, and *Mcp1* was detected in the distal colons by

qRT–PCR. Data are the means ± SDs. n = 6. *P<0.05, **P<0.01. **(C)** The protein levels of IL-1β, IL-6, MCP1, and ICAM1 were measured in serum by ELISAs. Data are the means ± SDs. n = 6. *P<0.05, **P<0.01, ***P<0.001, ****P<0.0001. **(D)** The protein levels of MMP9, p-P65, cl-caspase3, cl-caspase7, and PUMA detected by Western blots in mice. *P<0.05, **P<0.01. **(E)** Serum FITC–dextran levels of DSS-treated WT, *Olfm4*$^{-/-}$ mice, and *Olfm4* re-expression mice. Data are the means ± SDs. n = 6. *P<0.05, **P<0.01, ****P<0.0001. **(F)** Colon sections were stained with H&E (scale bar: 50 μm) to assess injury and inflammation. TUNEL staining showed apoptotic cells in the mouse colons (scale bar: 50 μm). **(G)** The mRNA expression of *Il1β*, *Icam1*, and *Mcp1* was detected in the distal colons by qRT–PCR. Data are the means ± SDs. n = 6. *P<0.05, **P<0.01, ***P<0.001. **(H)** The protein levels of IL-1β, IL-6, MCP1, and ICAM1 were measured in serum by ELISAs. Data are the means ± SDs. n = 6. *P<0.05, **P<0.01, ***P<0.001, ****P<0.0001. **(I)** Serum FITC–dextran levels of DSS-treated WT, *Olfm4*$^{-/-}$ mice, and p53 knockdown *Olfm4*$^{-/-}$ mice. Data are the means ± SDs. n = 6. *P<0.05, **P<0.01, ****P<0.0001. **(J)** The mRNA expression of *Il1β*, *Icam1*, and *Mcp1* was detected in HCT116 cells by qRT–PCR. Data are the means ± SDs. n = 6. *P<0.05, **P<0.01, ***P<0.001, ****P<0.0001.

As the downstream factor of Mmp9, Notch signaling is modulated by Mmp9 and regulates intestinal epithelial homeostasis [59]. Previous studies have suggested a potential relationship between *Olfm4* and Notch [74, 75]. Our results showed that *Olfm4* can regulate Notch1 rather than just being regulated. Knockdown of p53, reduction in Mmp9, or inhibition of Notch1 could reverse the exacerbation of colitis caused by *Olfm4* deletion. We observed a significant effect of *Olfm4* on the Mmp9-Notch1-p53 axis in colitis regulation. This axis was proposed in research on colitis-associated cancer [37, 38] but has never been assessed in colitis research.

Several limitations are acknowledged in this study. First, OLFM4 may regulate ulcerative colitis through a more complex mechanism than previously discovered. There is crosstalk between p53 and the NF-κB pathway [76]. The NF-κB transcription factor can both contribute to and, in other situations, protect against apoptosis [76, 77]. The exact role of NF-κB in apoptosis under the specific circumstances of this study needs further investigation. Moreover, other factors may contribute to the pathogenesis in our study. In addition, in our study, we focused more on its effects on pathogenic pathways and less on stem cell properties, which will be an important direction for our future research. Furthermore, because the *Olfm4*-/- mice used in this study were systemically knocked out, it is difficult to avoid the potential influence of OLFM4 in other organs, except the intestine. Therefore, intestinal epithelium-specific OLFM4 knockout mice are planned for future experiments. Finally, further studies are required to demonstrate the clinical application value of *Olfm4* in UC patients.

In conclusion, our results demonstrated that OLFM4 is significantly upregulated in UC, and OLFM4 targets MMP9 and regulates p53-mediated apoptosis via NOTCH1 signaling in experimental colitis. These findings suggest that OLFM4 may serve as a potential diagnostic marker and therapeutic target for UC.

Abbreviations

AAV: adeno-associated virus; ADP-ribose: apoptosis-related factors including cleaved of poly; ANOVA: analyses of variance; BCL2: B-cell lymphoma 2; BAX: BCL2-associated X protein; CD: Crohn's disease; co-IP: coimmunoprecipitation; DAPT: difluorophenacetyl-L-alanyl-S-phenylglycine t-butyl ester; DMEM: Dulbecco's modified Eagle's medium; DSS: dextran sulfate sodium; ECM: extracellular matrix; ELISA: enzyme-linked immunosorbent assay; FBS: fetal bovine serum; FPKM: fragments per kilobase of transcript per million fragments mapped; FITC: fluorescein isothiocyanate; GSEA: gene set enrichment analysis; HES1: hairy and enhancer of split-1; IBD: inflammatory bowel disease; Icam1: intercellular adhesion molecule-1; IEC: intestinal epithelial cells; Il6: interleukin-6; IHC: immunohistochemistry; IKK: IκB kinase; LPS: lipopolysaccharide; Mcp1: monocyte chemoattractant protein-1; MMP9: matrix metalloproteinase-9; Ngal-MMP9: neutrophil gelatinase B-associated lipocalin and MMP9; NF-κB: nuclear factor-κB; OLFM4: olfactomedin-4; PARP: polymerase; PUMA: p53 upregulated modulator of apoptosis; PBS: phosphate-buffered saline; RPMI: Roswell Park Memorial Institute; SD: standard deviation; SPF: specific pathogen-free; TUNEL: triphosphate nick-end labeling; UC: ulcerative colitis; WT: wild type.

Supplementary Material

Supplementary figures and tables.
https://www.ijbs.com/v19p2150s1.pdf

Acknowledgments

The authors thank the editors of AJE (www.aje.com) for their linguistic assistance in English language editing and proofreading (Certificate Verification Key: 20D5-9682-CD24-E5DF-E691).

Funding

This work was supported by the National Key Research and Development Program (2018YFA0109800) and the National Natural Science Foundation of China (81470838, 81770573, 81870400, 82070585).

Author contributions

XW and SC contributed equally to this investigation, acquisition of data and drafting of the article. JW, YC and YG provided support in the conception and design of the study. QW, ZL and GZ contributed to the analysis and interpretation of data. CX led the study and critically revised the article. All

the authors approved the final version to be submitted.

Data sharing statement

All data relevant to this study are included in the manuscript or uploaded as supplementary information. The data are available in a public, open access repository to other researchers.

Competing Interests

The authors have declared that no competing interest exists.

References

1. Kobayashi T, Siegmund B, Le Berre C, et al. Ulcerative colitis. Nat Rev Dis Primers 2020;6:74.
2. Xavier RJ, Podolsky DK. Unravelling the pathogenesis of inflammatory bowel disease. Nature 2007;448:427-34.
3. Famularo G, Trinchieri V, De Simone C. Inflammatory bowel disease. N Engl J Med 2002;347:1982-4; author reply 1982-4.
4. de Souza HS, Fiocchi C. Immunopathogenesis of IBD: current state of the art. Nat Rev Gastroenterol Hepatol 2016;13:13-27.
5. Tatiya-Aphiradee N, Chatuphonprasert W, Jarukamjorn K. Immune response and inflammatory pathway of ulcerative colitis. J Basic Clin Physiol Pharmacol 2018;30:1-10.
6. Neurath MF. Cytokines in inflammatory bowel disease. Nat Rev Immunol 2014;14:329-42.
7. Peterson LW, Artis D. Intestinal epithelial cells: regulators of barrier function and immune homeostasis. Nat Rev Immunol 2014;14:141-53.
8. Qiu W, Wu B, Wang X, et al. PUMA-mediated intestinal epithelial apoptosis contributes to ulcerative colitis in humans and mice. J Clin Invest 2011;121:1722-32.
9. Kiesslich R, Duckworth C, Moussata D, et al. Local barrier dysfunction identified by confocal laser endomicroscopy predicts relapse in inflammatory bowel disease. Gut 2012;61:1146-53.
10. Ivanov AI. Structure and regulation of intestinal epithelial tight junctions: current concepts and unanswered questions. Adv Exp Med Biol 2012;763:132-48.
11. Stange EF, Schroeder BO. Microbiota and mucosal defense in IBD: an update. Expert Rev Gastroenterol Hepatol 2019;13:963-976.
12. Lin W, Ma C, Su F, et al. Raf kinase inhibitor protein mediates intestinal epithelial cell apoptosis and promotes IBDs in humans and mice. Gut 2017;66:597-610.
13. Martini E, Krug SM, Siegmund B, et al. Mend Your Fences: The Epithelial Barrier and its Relationship With Mucosal Immunity in Inflammatory Bowel Disease. Cell Mol Gastroenterol Hepatol 2017;4:33-46.
14. Zhang J, Liu WL, Tang DC, et al. Identification and characterization of a novel member of olfactomedin-related protein family, hGC-1, expressed during myeloid lineage development. Gene 2002;283:83-93.
15. Wang XY, Chen SH, Zhang YN, et al. Olfactomedin-4 in digestive diseases: A mini-review. World J Gastroenterol 2018;24:1881-1887.
16. Grover PK, Hardingham JE, Cummins AG. Stem cell marker olfactomedin 4: critical appraisal of its characteristics and role in tumorigenesis. Cancer Metastasis Rev 2010;29:761-75.
17. Liu W, Rodgers GP. Olfactomedin 4 expression and functions in innate immunity, inflammation, and cancer. Cancer Metastasis Rev 2016;35:201-12.
18. Liu W, Lee HW, Liu Y, et al. Olfactomedin 4 is a novel target gene of retinoic acids and 5-aza-2'-deoxycytidine involved in human myeloid leukemia cell growth, differentiation, and apoptosis. Blood 2010;116:4938-47.
19. Liu W, Yan M, Liu Y, et al. Olfactomedin 4 down-regulates innate immunity against Helicobacter pylori infection. Proc Natl Acad Sci U S A 2010;107:11056-61.
20. Liu W, Chen L, Zhu J, et al. The glycoprotein hGC-1 binds to cadherin and lectins. Exp Cell Res 2006;312:1785-97.
21. Shinozaki S, Nakamura T, Iimura M, et al. Upregulation of Reg 1alpha and GW112 in the epithelium of inflamed colonic mucosa. Gut 2001;48:623-9.
22. van der Flier LG, Haegebarth A, Stange DE, et al. OLFM4 is a robust marker for stem cells in human intestine and marks a subset of colorectal cancer cells. Gastroenterology 2009;137:15-7.
23. Gersemann M, Becker S, Nuding S, et al. Olfactomedin-4 is a glycoprotein secreted into mucus in active IBD. J Crohns Colitis 2012;6:425-434.
24. Nagase H, Visse R, Murphy G. Structure and function of matrix metalloproteinases and TIMPs. Cardiovasc Res 2006;69:562-73.
25. Wilhelm SM, Collier IE, Marmer BL, et al. SV40-transformed human lung fibroblasts secrete a 92-kDa type IV collagenase which is identical to that secreted by normal human macrophages. J Biol Chem 1989;264:17213-21.
26. Opdenakker G, Van den Steen PE, Dubois B, et al. Gelatinase B functions as regulator and effector in leukocyte biology. J Leukoc Biol 2001;69:851-9.
27. Vandooren J, Van den Steen PE, Opdenakker G. Biochemistry and molecular biology of gelatinase B or matrix metalloproteinase-9 (MMP-9): the next decade. Crit Rev Biochem Mol Biol 2013;48:222-72.
28. Arihiro S, Ohtani H, Hiwatashi N, et al. Vascular smooth muscle cells and pericytes express MMP-1, MMP-9, TIMP-1 and type I procollagen in inflammatory bowel disease. Histopathology 2001;39:50-9.
29. Matsuno K, Adachi Y, Yamamoto H, et al. The expression of matrix metalloproteinase matrilysin indicates the degree of inflammation in ulcerative colitis. J Gastroenterol 2003;38:348-54.
30. de Bruyn M, Arijs I, De Hertogh G, et al. Serum Neutrophil Gelatinase B-associated Lipocalin and Matrix Metalloproteinase-9 Complex as a Surrogate Marker for Mucosal Healing in Patients with Crohn's Disease. J Crohns Colitis 2015;9:1079-87.
31. de Bruyn M, Arijs I, Wollants WJ, et al. Neutrophil gelatinase B-associated lipocalin and matrix metalloproteinase-9 complex as a surrogate serum marker of mucosal healing in ulcerative colitis. Inflamm Bowel Dis 2014;20:1198-207.
32. Meek DW. Tumour suppression by p53: a role for the DNA damage response? Nat Rev Cancer 2009;9:714-23.
33. Spehlmann ME, Manthey CF, Dann SM, et al. Trp53 deficiency protects against acute intestinal inflammation. J Immunol 2013;191:837-47.
34. Goretsky T, Dirisina R, Sinh P, et al. p53 mediates TNF-induced epithelial cell apoptosis in IBD. Am J Pathol 2012;181:1306-15.
35. Merritt AJ, Allen TD, Potten CS, et al. Apoptosis in small intestinal epithelial from p53-null mice: evidence for a delayed, p53-independent G2/M-associated cell death after gamma-irradiation. Oncogene 1997;14:2759-66.
36. Dirisina R, Katzman RB, Goretsky T, et al. p53 and PUMA independently regulate apoptosis of intestinal epithelial cells in patients and mice with colitis. Gastroenterology 2011;141:1036-45.
37. Walter L, Canup B, Pujada A, et al. Matrix metalloproteinase 9 (MMP9) limits reactive oxygen species (ROS) accumulation and DNA damage in colitis-associated cancer. Cell Death Dis 2020;11:767.
38. Garg P, Jeppsson S, Dalmasso G, et al. Notch1 regulates the effects of matrix metalloproteinase-9 on colitis-associated cancer in mice. Gastroenterology 2011;141:1381-92.
39. Ordas I, Eckmann L, Talamini M, et al. Ulcerative colitis. Lancet 2012;380:1606-19.
40. Huang LY, He Q, Liang SJ, et al. ClC-3 chloride channel/antiporter defect contributes to inflammatory bowel disease in humans and mice. Gut 2014;63:1587-95.
41. Siegmund B, Lehr H-A, Fantuzzi G, et al. IL-1β-converting enzyme (caspase-1) in intestinal inflammation. Proc Natl Acad Sci U S A 2001;98:13249-13254.
42. Zhang J, Xu M, Zhou W, et al. Deficiency in the anti-apoptotic protein DJ-1 promotes intestinal epithelial cell apoptosis and aggravates inflammatory bowel disease via p53. J Biol Chem 2020;295:4237-4251.
43. Polyak S, Mach A, Porvasnik S, et al. Identification of adeno-associated viral vectors suitable for intestinal gene delivery and modulation of experimental colitis. Am J Physiol Gastrointest Liver Physiol 2012;302:G296-308.
44. Hasbrouck NC, High KA. AAV-mediated gene transfer for the treatment of hemophilia B: problems and prospects. Gene Ther 2008;15:870-5.
45. Zhang H, Shen Z, Lin Y, et al. Vitamin D receptor targets hepatocyte nuclear factor 4α and mediates protective effects of vitamin D in nonalcoholic fatty liver disease. J Biol Chem 2020;295:3891-3905.
46. Fang Y, Shen ZY, Zhan YZ, et al. CD36 inhibits β-catenin/c-myc-mediated glycolysis through ubiquitination of GPC4 to repress colorectal tumorigenesis. Nat Commun 2019;10:3981.
47. Liu L, Tao T, Liu S, et al. An RFC4/Notch1 signaling feedback loop promotes NSCLC metastasis and stemness. Nat Commun 2021;12:2693.
48. Hans CP, Sharma N, Dev R, et al. DAPT, a potent Notch inhibitor regresses actively growing abdominal aortic aneurysm via divergent pathways. Clin Sci (Lond) 2020;134:1555-1572.
49. Dovey HF, John V, Anderson JP, et al. Functional gamma-secretase inhibitors reduce beta-amyloid peptide levels in brain. J Neurochem 2001;76:173-81.
50. Zhu G, Cheng Z, Lin C, et al. MyD88 Regulates LPS-induced NF-κB/MAPK Cytokines and Promotes Inflammation and Malignancy in Colorectal Cancer Cells. Cancer Genomics Proteomics 2019;16:409-419.
51. Yuan T, Zhang L, Yao S, et al. miR-195 promotes LPS-mediated intestinal epithelial cell apoptosis via targeting SIRT1/eIF2a. Int J Mol Med 2020;45:510-518.
52. Shabani S, Mahjoubi F, Moosavi MA. A siRNA-based method for efficient silencing of PYROXD1 gene expression in the colon cancer cell line HCT116. J Cell Biochem 2019;120:19310-19317.
53. Tabatabaei MS, Ahmed M. Enzyme-Linked Immunosorbent Assay (ELISA). Methods Mol Biol 2022;2508:115-134.
54. Dirisina R, Katzman R, Goretsky T, et al. p53 and PUMA independently regulate apoptosis of intestinal epithelial cells in patients and mice with colitis. Gastroenterology 2011;141:1036-45.
55. Liu Y, Peng J, Sun T, et al. Epithelial EZH2 serves as an epigenetic determinant in experimental colitis by inhibiting TNFα-mediated inflammation and apoptosis. Proc Natl Acad Sci U S A 2017;114:E3796-e3805.
56. Baeuerle PA HT. Function and activation of NF-kB in the immune system. Annu Rev Immunol 1994;12:141–179.

57. Lawrence T. The nuclear factor NF-kappaB pathway in inflammation. Cold Spring Harb Perspect Biol 2009;1:a001651.
58. Riley T, Sontag E, Chen P, et al. Transcriptional control of human p53-regulated genes. Nat Rev Mol Cell Biol 2008;9:402-12.
59. Pope JL, Bhat AA, Sharma A, et al. Claudin-1 regulates intestinal epithelial homeostasis through the modulation of Notch-signalling. Gut 2014;63:622-34.
60. Roemer K. Notch and the p53 clan of transcription factors. Adv Exp Med Biol 2012;727:223-40.
61. Nakamura T, Tsuchiya K, Watanabe M. Crosstalk between Wnt and Notch signaling in intestinal epithelial cell fate decision. J Gastroenterol 2007;42:705-10.
62. Okayasu I, Hatakeyama S, Yamada M, et al. A novel method in the induction of reliable experimental acute and chronic ulcerative colitis in mice. Gastroenterology 1990;98:694-702.
63. Wirtz S, Neurath MF. Mouse models of inflammatory bowel disease. Adv Drug Deliv Rev 2007;59:1073-83.
64. Takagawa T, Kitani A, Fuss I, et al. An increase in LRRK2 suppresses autophagy and enhances Dectin-1-induced immunity in a mouse model of colitis. Sci Transl Med 2018;10: eaan8162.
65. Vallabhapurapu S, Karin M. Regulation and function of NF-kappaB transcription factors in the immune system. Annu Rev Immunol 2009;27:693-733.
66. Liu Y, Wang K, Liang X, et al. Complement C3 Produced by Macrophages Promotes Renal Fibrosis via IL-17A Secretion. Front Immunol 2018;9:2385.
67. Atreya I, Atreya R, Neurath MF. NF-kappaB in inflammatory bowel disease. J Intern Med 2008;263:591-6.
68. Wan Y, Yang L, Jiang S, et al. Excessive Apoptosis in Ulcerative Colitis: Crosstalk Between Apoptosis, ROS, ER Stress, and Intestinal Homeostasis. Inflamm Bowel Dis 2022;28:639-648.
69. Martens S, Bridelance J, Roelandt R, et al. MLKL in cancer: more than a necroptosis regulator. Cell Death Differ 2021;28:1757-1772.
70. Tang R, Xu J, Zhang B, et al. Ferroptosis, necroptosis, and pyroptosis in anticancer immunity. J Hematol Oncol 2020;13:110.
71. Du J, Yin J, Du H, et al. Revisiting an Expression Dataset of Discordant Inflammatory Bowel Disease Twin Pairs Using a Mutation Burden Test Reveals CYP2C18 as a Novel Marker. Front Genet 2021;12:680125.
72. Liu W, Li H, Hong SH, et al. Olfactomedin 4 deletion induces colon adenocarcinoma in Apc(Min/+) mice. Oncogene 2016;35:5237-5247.
73. Al-Sadi R, Youssef M, Rawat M, et al. MMP-9-induced increase in intestinal epithelial tight permeability is mediated by p38 kinase signaling pathway activation of MLCK gene. Am J Physiol Gastrointest Liver Physiol 2019;316:G278-g290.
74. Kuno R, Ito G, Kawamoto A, et al. Notch and TNF-α signaling promote cytoplasmic accumulation of OLFM4 in intestinal epithelium cells and exhibit a cell protective role in the inflamed mucosa of IBD patients. Biochem Biophys Rep 2021;25:100906.
75. VanDussen KL, Carulli AJ, Keeley TM, et al. Notch signaling modulates proliferation and differentiation of intestinal crypt base columnar stem cells. Development 2012;139:488-97.
76. Carrà G, Lingua MF, Maffeo B, et al. P53 vs NF-κB: the role of nuclear factor-kappa B in the regulation of p53 activity and vice versa. Cell Mol Life Sci 2020;77:4449-4458.
77. Foo SY, Nolan GP. NF-kappaB to the rescue: RELs, apoptosis and cellular transformation. Trends Genet 1999;15:229-35.